Preparation of Boron and Boron Phosphide Films by Photo- and Thermal Chemical Vapor Deposition Processes

Y. Kumashiro, K. Sato, S. Chiba, S. Yamada, D. Tanaka, K. Hyodo, T. Yokoyama, and K. Hirata

Faculty of Engineering, Yokohama National University, 79-5 Tokiwadai, Hodogaya-ku Yokohama-shi, 240-8501, Japan

We have calculated first excitation energies, oscillator strengths, and potential energy surfaces of B_2H_6 and PH_3 by using an *ab initio* molecular orbital method to confirm that the deuterium lamp is effective for the excitation of both B_2H_6 and PH_3 in the photo-chemical vapor deposition (photo-CVD) process. The deuterium lamp is useful for growing the film at 600–1000°C in the B_2H_6–PH_3–H_2 system. The activation energies for film growth for thermal CVD decrease by using the deuterium lamp. Boron phosphide film grew epitaxially on Si(100) plane with a deuterium lamp at lower temperature than by thermal CVD at 100°C. The electrical properties of boron and boron phosphide films on silica glass were improved by deuterium. © 2000 Academic Press

INTRODUCTION

The main features of boron and boron compound semiconductors are a large neutron cross section of ^{10}B and high thermoelectric power, which make them applicable for neutron detectors or high-temperature thermoelectric devices. For these purposes we have been preparing boron-based semiconductors by chemical vapor deposition (CVD) and molecular beam deposition (MBD) and measuring electrical properties to clarify promising electronic applications.

Boron phosphide single crystals prepared by CVD contain autodoped Si from substrate due to high-temperature growth, which prohibits high resistivity and high mobility by reducing carrier concentration.

On the other hand boron phosphide prepared by MBD has high resistivity but is amorphous with high phosphorus-deficient composition to form various trap levels.

The application of laser and lamp radiation to the growth of high-quality elements and compound films is referred to as photo-CVD, and has been tried in the epitaxial growth of silicon from $SiCl_4$ diluted in H_2 with mercury lamp irradiation (1) and photoexcited epitaxial growth of GaAs (2). Interest in photo-CVD comes from the ability of optical radiation to induce specific chemical reactions in the gas or

at a surface. The photodeposition of film permits operation at lower temperatures, where impurity redistribution and thermally induced mechanical stress are minimized. Then the photoexcited process has the potential to reduce growth temperature and to improve the quality of films (3).

There is one work on 193-nm excimer-laser irradiation in boron CVD films from B_2H_6 + He indicatig a photochemically enhanced growth reaction (4).

We have prepared boron and boron phosphide films with good crystal quality with the aid of a photo-CVD process. The range of the lamp, the first excitation energies, the oscillator strength, and potential energy surfaces were calculated by using the *ab initio* molecular orbital method (5). We selected a deuterium lamp with radiation wavelength of 115–400 nm. The films were grown on a Si(100) plane and silica glass with and without a lamp at various growth temperatures to evaluate crystal quality by X-ray diffraction (XRD) and reflection high-electron-energy diffraction (RHEED) and electrical properties by the van der Pauw method.

THEORETICAL CALCULATION

Diborane has a continuous absorption region between 210 and 180 nm with a maximum at 183 nm (6, 7). The primary photoprocess is suggested (6, 7) to be

$$B_2H_6 + h\nu \rightarrow B_2H_5 + H. \qquad [1]$$
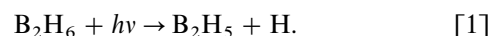
The primary photoprocess at 193 nm is

$$B_2H_6 + h\nu \rightarrow BH_3 + BH_3. \qquad [2]$$
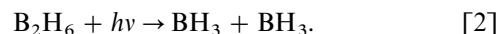
Komatsu *et al.* (4) found direct evidence to indicate the photochemically enhanced growth reaction of boron from B_2H_6 by 193-nm excimer-laser irradiation.

Phosphine also absorbs strongly in the vacuum ultra-violet (VUV), with absorption maxima occurring in the region 180–200 nm (8). The absorption spectra are continuous. The primary photoprocess is molecular

TABLE 1
Properties of Excited States of B_2H_6 and PH_3

	Excitation energy (eV)	Absorption wavelength (nm)	Decomposition mode	Oscillator strength (a.u)
B_2H_6				
1st excited state	8.42	147.2	No decomposition	0
2nd excited state	9.42	131.7	$BH_2 + BH_4$	0
3rd excited state	9.94	124.7	No decomposition	0
4th excited state	11.56	107.3	$2BH_3$	0.4634
5th excited state	12.20	101.6	No decomposition	0.0011
6th excited state	13.15	94.3	$2BH_3$	0.0042
PH_3				
1st excited state	8.04	154.3	$PH + 2H$	0.1858
2nd excited state	8.04	154.3	$PH + 2H$	0.1858
3rd excited state	10.27	120.7	$PH_2 + H$	0.1750

dissociation,

$$PH_3 + h\nu \rightarrow PH_2(\bar{A}(^2A_1)) + H$$

$$PH_2(\bar{X}(^2B_1)) + H, \qquad [3]$$
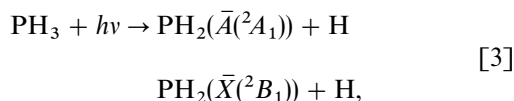
where only $\sim 1\%$ of the PH_2 radicals are produced in the excited ($\bar{A}$) state; most are formed directly in the ground state.

To determine the lamp below 150 nm, first excitation energies, oscillator strengths, and potential energy surfaces of B_2H_6 and PH_3 were calculated by using an *ab initio* molecular orbital method (9). The single-excitation C1 method (10) was used to obtain each excited state. An A6-31G* basis set and Gaussian 94 program were used for the calculation. Properties of excited states of B_2H_6 and PH_3 are listed in Table 1.

The energies for the lowest excitation with considerable oscillator strength were calculated to be 8.0 and 11.6 eV for PH_3 and B_2H_6, respectively. The absorption wavelength for reactant gases indicates that readiness for decomposition of B_2H_6 is effective to 107.3 nm and that of PH_3 is 120.7 and 154.3 nm. The VUV absorption spectrum of B_2H_6 (6) could not detect the absorption at 107.3 nm. In the absorption of PH_3 (11) the first continuum starts with a very low absorption near 230.0 nm. A second start is observed in the region 159.2–149 nm. The resolution was not sufficient to resolve the vibration structure at 154 nm. The emission from PH begins at 159 ± 2 nm, where the signal is very low, but a sharp increase appears at about 121.0 ± 1 nm. The emission attributed to PH_2 begins at 208 ± 1 nm and extends down to about 120 nm (11).

We selected a deuterium lamp with a radiation wavelength of 115–400 nm. As the calculated excitation energies tend to be slightly higher than the observed values,

the deuterium lamp is considered to be effective for the excitation of both B_2H_6 and PH_3.

A deuterium lamp produces neglible radiation in the visible but generates peaks near $\lambda = 180$ nm (11). Deuterium lamps having average power up to 60 W are readily available so they play an important role in photoassisted deposition processes.

EXPERIMENTAL

The reactant gases B_2H_6 (1% in hydrogen) and PH_3 (5% in hydrogen) were used. The CVD furnace is modified by a thermal CVD furnace (12), equipped with a deuterium lamp (Fig. 1). To introduce the radiation from the deuterium lamp into the reactor, an entrance window must be provided on the condition that the material should offer maximum transmission at short wavelengths. MgF_2 was selected because the "cutoff" wavelength is 110 nm and its transmission increases up to 60% at 125 nm to become constant up
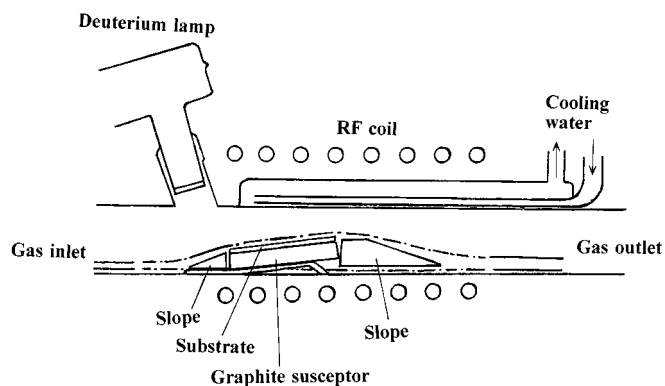
FIG. 1. CVD furnace equipped with deuterium lamp.

to 140 nm and increases up to 160 nm with 80% transmission (11).

After heat treatment of the substrate (12), the two reactant gases were mixed with hydrogen at the growth temperature. Growth occurred at gas flow rates of 20, 500, and 2500 cm^3/min for diborane, phosphine, and hydrogen, respectively, in the temperature range 600 to 1000°C at a deposition time of 1 h with and without the deuterium lamp.

The films were characterized by XRD and RHEED patterns. Ohmic contacts of the films were made by evaporated Al, followed by annealing in argon at 400°C. Electrical properties of the films at room temperature were measured by the van der Pauw method.

RESULTS AND DISCUSSION

A. Boron Films

Boron films obtained with the B_2H_6 and H_2 mixture show amorphous structures. SEM of the films (Fig. 2) indicate that the round grain increases up to 0.5–2.5 μm in diameter with smooth surfaces with an increase in growth temperature.

The growth rates and reciprocal temperatures are shown in Fig. 3. The activation energy of 14.3 kJ/mol for thermal CVD decreases to 4.1 kJ/mol by using photo-CVD, which demonstrates the decomposition and excitation of B_2H_6 by the deuterium lamp. In the case of thermal CVD, B_2H_6
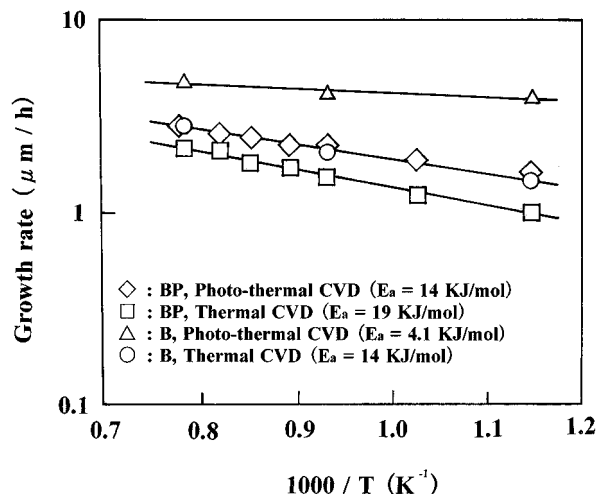
FIG. 3. Relationship between growth rates and reciprocal temperatures.

dissociates completely into BH_3 molecules at the growth temperature (13). In addition to photo-CVD process, promotion of decomposition and excitation for B_2H_6 (Table 1) is enhanced by the deuterium lamp.

The transition of B_2H_6 to the fourth excitation state is within the range of the emission wavelength of deuterium and has high oscillating strength, which would produce a high growth rate with low activation energy. The electrical

Plot legend:
◇ : BP, Photo-thermal CVD (E$_a$ = 14 KJ/mol)
□ : BP, Thermal CVD (E$_a$ = 19 KJ/mol)
△ : B, Photo-thermal CVD (E$_a$ = 4.1 KJ/mol)
○ : B, Thermal CVD (E$_a$ = 14 KJ/mol)

600°C   800°C   1000°C
Photo-thermal CVD

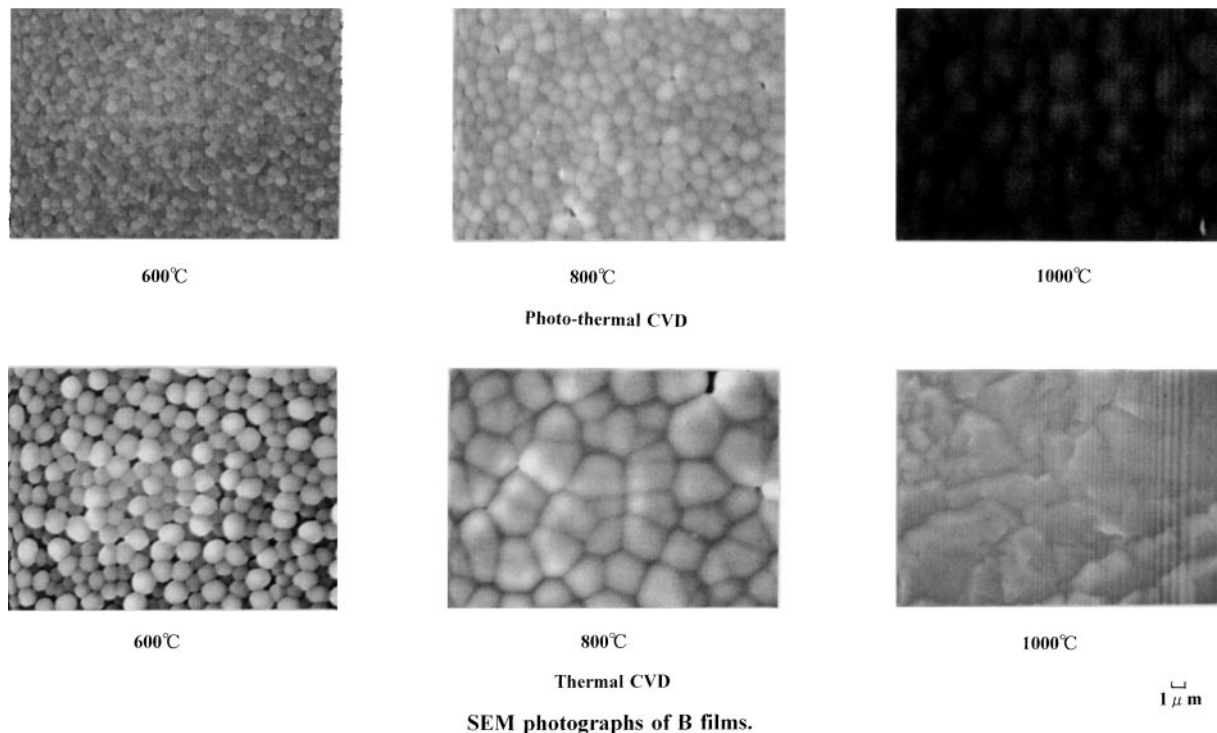600°C   800°C   1000°C
Thermal CVD

SEM photographs of B films.

FIG. 2. SEM observations of boron films.

properties of film grown on silica glass at room temperature with and without photo-CVD are shown in Fig. 4. All boron films are p-type conductors. Photothermal CVD boron tends to have higher mobility and lower carrier concentrations than thermal CVD boron, although there is not a great difference in the electrical properties between the two processes at 1000°C.

B. Boron Phosphide

A Noticeable difference in the XRD patterns of boron phosphide films grown on a Si(100) plane with and without irradiation from the deuterium lamp is observed at growth temperatures between 600 and 1000°C so there is no experimental deposition below 600°C and above 1000°C. The boron phosphide film grown at 600°C shows an amorphous structure with a broad peak in XRD. The film grown at 1000°C shows a textured RHEED pattern. A temperature of 600°C would provide insufficient energy to grow film by irradiation but 1000°C would be enough thermal energy to grow film without irradiation. The pattern changes at the growth temperature of 800°C. The XRD of boron phosphide prepared by thermal CVD shows a polycrystalline struc-

ture with various orientations, but that prepared by irradiation with the deuterium lamp orients predominately on the (100) plane (Fig. 5).

The RHEED patterns of these films are shown in Fig. 6A. The best RHEED patterns are obtained by photothermal CVD at 850°C (Fig. 6B), indicating that the RHEED pattern at [110] incident direction is the same as at [100] incident direction energy 45° rotation in the (100) plane. The epitaxial relationships between Si(100) and BP(100) are

$$BP(100) [100] // Si(100) [100],$$

$$BP(100) [110] // Si(100) [110].$$

Thus boron phosphide grows epitaxially at lower temperature than the thermal CVD process for 950°C (12).

The activation energy of 19.3 kJ/mol decreases slightly to 14.3 kJ/mol by using photo-CVD (Fig. 3), which demonstrates that the decomposition and excitation of PH_3 by deuterium are not so appreciable as for B_2H_6. This is consistent with low formation of PH_2 radical in formula [3]. The oscillating strength of PH would be expected to be almost same as that of PH (Table 1) so the degree of formation of the radicals in PH_3 is low in comparison with B_2H_6. Despite these facts, the experimental result that BP grows epitaxially on a Si(100) plane at lower temperature than thermal CVD would be due to new reaction mechanism by deuterium irradiation.

In addition to the promotion of decomposition in the reactant gases, the following effects would be probable in photoassisted CVD. The method of decomposing the reactant gases would vary the reactant precursor to reduce the activation energy. Hydrogen gas as a carrier would decompose into hydrogen radicals by deuterium lamp or the
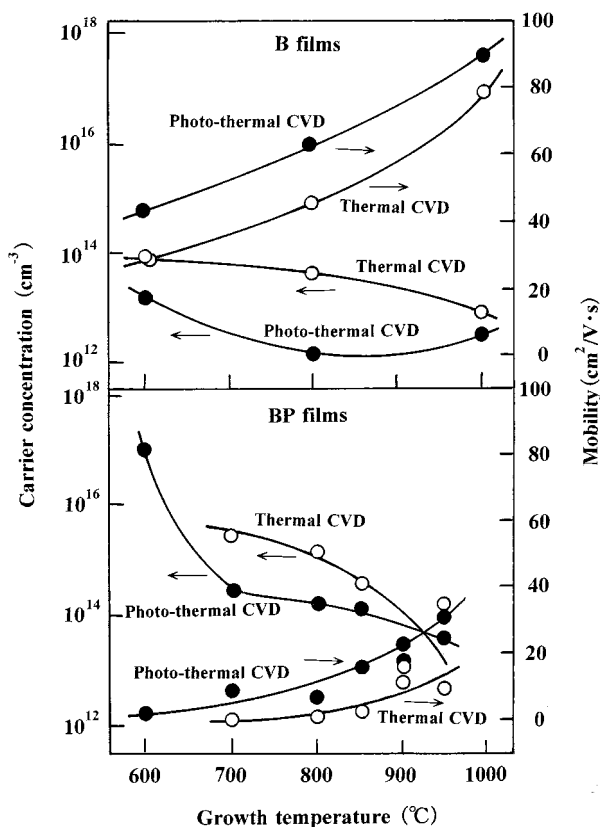

FIG. 4. Electrical properties of boron and boron phosphide films grown on silica glass at various growth temperatures.
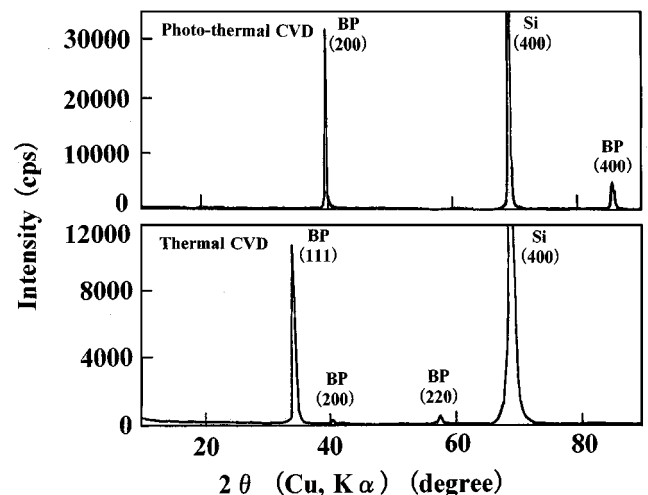

FIG. 5. X-Ray diffraction patterns of BP films on Si(100) planes by thermal and photothermal CVD processes.
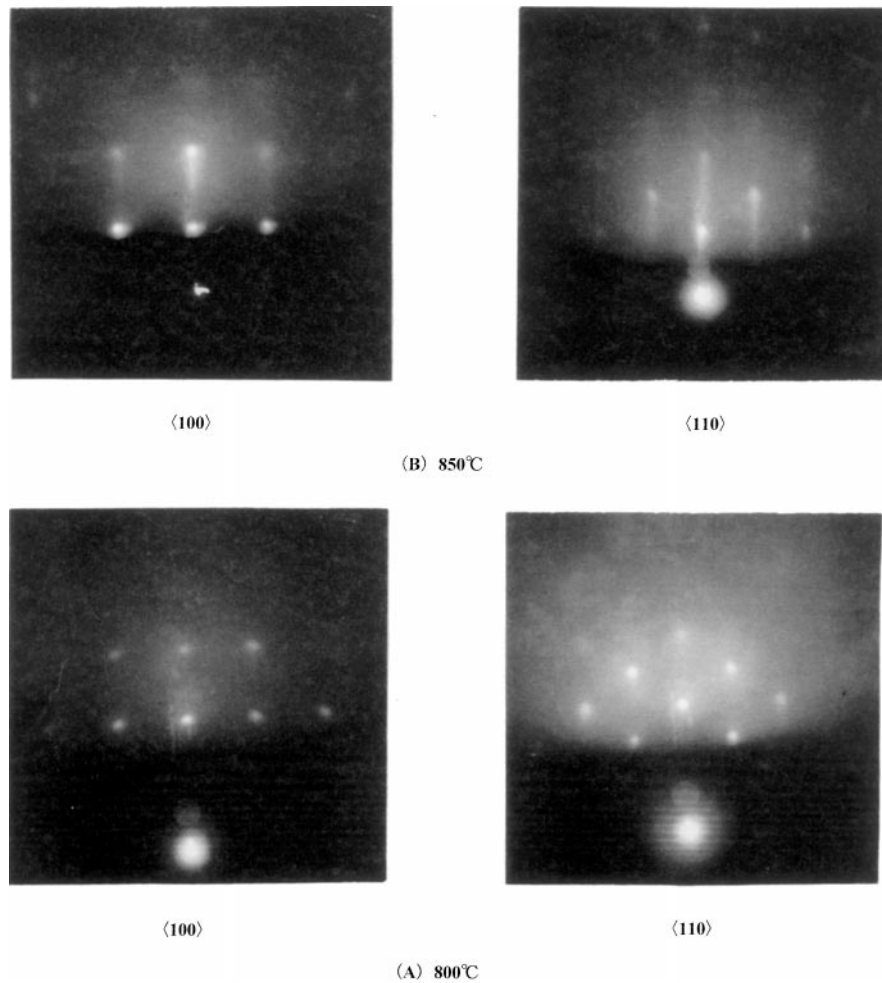
FIG. 6. RHEED patterns of BP films on Si(100) planes grown at 800°C (A) and 850°C (B).

hydrogen radicals would increase with the promotion of both diborane and phosphine decompositions to abstract the hydrogen on the surface of the substrate so formation of BP films would be favored by combining such active molecules as BH_3 and PH_3.

The content of boron in the film determined by X-ray photoelectron spectroscopy (XPS) is higher at the growth temperature of 600°C, but it decreases with a rise in growth temperature. The phosphorus content of photothermal film is higher than that of thermal film, which becomes conspicuous at high temperatures. The film with high phosphorus content shows good crystal quality. However, the films are all boron rich in boron phosphide, suggesting that boron aggregation forms a B_{12} cluster (14).

The electrical properties of boron phosphide films on silica glass with and without a deuterium lamp are also shown in Fig. 4. X-Ray diffraction patterns of the BP films on silica glass grown above 800°C show polycrystalline structures, but those below 750°C are amorphous. In the former case, strong BP(111), BP(200), and BP(200) planes

are observed for photothermal CVD film while only weak (111) and (200) planes are observed in thermal CVD film. Thus crystal distortion of the photothermal CVD film is less than that of the thermal film. Thermal CVD BP films grown at 600°C contain many structural disorders due to low growth temperature, so we could not measure the Hall effect due to high resistivity.

The conduction types of boron phosphide are determined by excess boron or phosphorus as *p* or *n*, respectively (15,16). In the present films, boron aggregation into B_{12} clusters would an form intrinsic acceptor level in the bandgap due to electron deficiency (17) showing *p*-type conduction. The mobility is enhanced by irradiation of deuterium at the same growth temperature. Although the photothermal CVD film tends to have lower carrier concentration than thermal CVD film, there is an exception for film grown at 900°C. The differences between them are small for the growth temperature of 850°C but the photothermal CVD film has a higher carrier concentration than the thermal film for 900°C growth. In considering small differences

in mobility at this growth temperature and phosphorus content for the photothermal CVD film is high for the growth temperature above 850°C in comparison with other growth temperatures, the specimen would be transient region from *p*- to *n*-type conductors. Of course, some complex reaction mechanism, grain boundary, and evaporation of phosphorus should be considered.

CONCLUSION

Boron and boron phosphide films have been prepared with the aid of photo-CVD by B_2H_6–PH_3–H_2 systems to grow good crystals quality. According to an *ab initio* molecular orbital method, the absorption wavelength for reactant gases indicates that promotion of decomposition of B_2H_6 is effective to 107.3 nm and that of PH_3 to 120.7 and 154.3 nm. The activation energy of boron film of 6.6 kJ/mol for thermal CVD decreases to 14.3 kJ/mol by using a deuterium lamp. Photothermal CVD boron films have lower hole concentration and higher mobility than thermal CVD boron films. No differences in the X-ray diffraction patterns of boron phosphide films on a Si(100) plane with and without irradiation by the deuterium lamp are observed at growth temperatures below 600°C and above 1000°C. The RHEED pattern of the boron phosphide film prepared with a deuterium lamp at 850°C shows the same pattern at the incident directions of [100] and [110] every 45° rotation in the (100) plane, indicating that boron phosphide grows epitaxially at lower temperature than with thermal CVD. The electrical properties of these films on silica glass are improved by photothermal CVD.

REFERENCES

1. M. Kumagawa, H. Sunami, T. Terasaki, and J. Nishizawa, *Jpn. Appl. Phys.* **7,** 1332 (1968).
2. J. Nishizawa, H. Abe, T. Kurabayashi, and M. Sakurai, *J. Vac. Sci. Technol. A* **4,** 706 (1986).
3. J. Nishizawa, *J. Cryst. Growth* **115,** 12 (1991).
4. S. Komatsu, M. Kasamatsu, K. Yamada, and Y. Moriyoshi, *J. Appl. Phys.* **71,** 5654 (1992).
5. K. Sato, D. Tanaka, and Y. Kumashiro, *in* "Proceedings, International Symposium on Electron–Molecule Collisions Swarms," in press.
6. M. P. Irion and K. L. Kompa, *J. Chem. Phys.* **76,** 2338 (1982).
7. J. G. Clark and R. G. Anderson, *Appl. Phys. Lett.* **32,** 46 (1978).
8. M. Rothschild, *in* "Laser Microfabrication Thin Film Process and Lithography" (D. J. Ehrlich and J. Y. Tsao, Eds.), p. 163, Academic Press, New York, 1989.
9. C. C. Roothaan, *Rev. Mod. Phys.* **23,** 69 (1951).
10. J. B. Foresman, M.-H. Gordon, J. A. Pople, and M. J. Frisch, *J. Phys. Chem.* **96,** 135 (1992).
11. J. G. Eden, *in* "Thin Film Processes II" (J. L. Vossen and W. Kern, Eds.), p. 611, Academic Press, San Diego, 1991.
12. Y. Kumashiro, Y. Okada, and H. Okumura, *J. Cryst. Growth* **132,** 611 (1993).
13. K. Shohno and H. Ohtake, *J. Cryst. Growth* **45,** 187 (1978).
14. K. Sato, N. Kanda, T. Ogata, and Y. Kumashiro, *Chem. Phys. Lett.*, in press (2000).
15. K. Shohno, M. Takigawa, and T. Nakada, *J. Cryst. Growth* **24/25,** 193 (1974).
16. Y. Kumashiro, *J. Mater. Res.* **5,** 2933 (1989).
17. H. Werheit, *in* "Electrical Refractory Materials" (Y. Kumashiro, Ed.), p. 589, Marcel Dekker, New York, 2000.